Supplementary Materials

Figures S1-S14

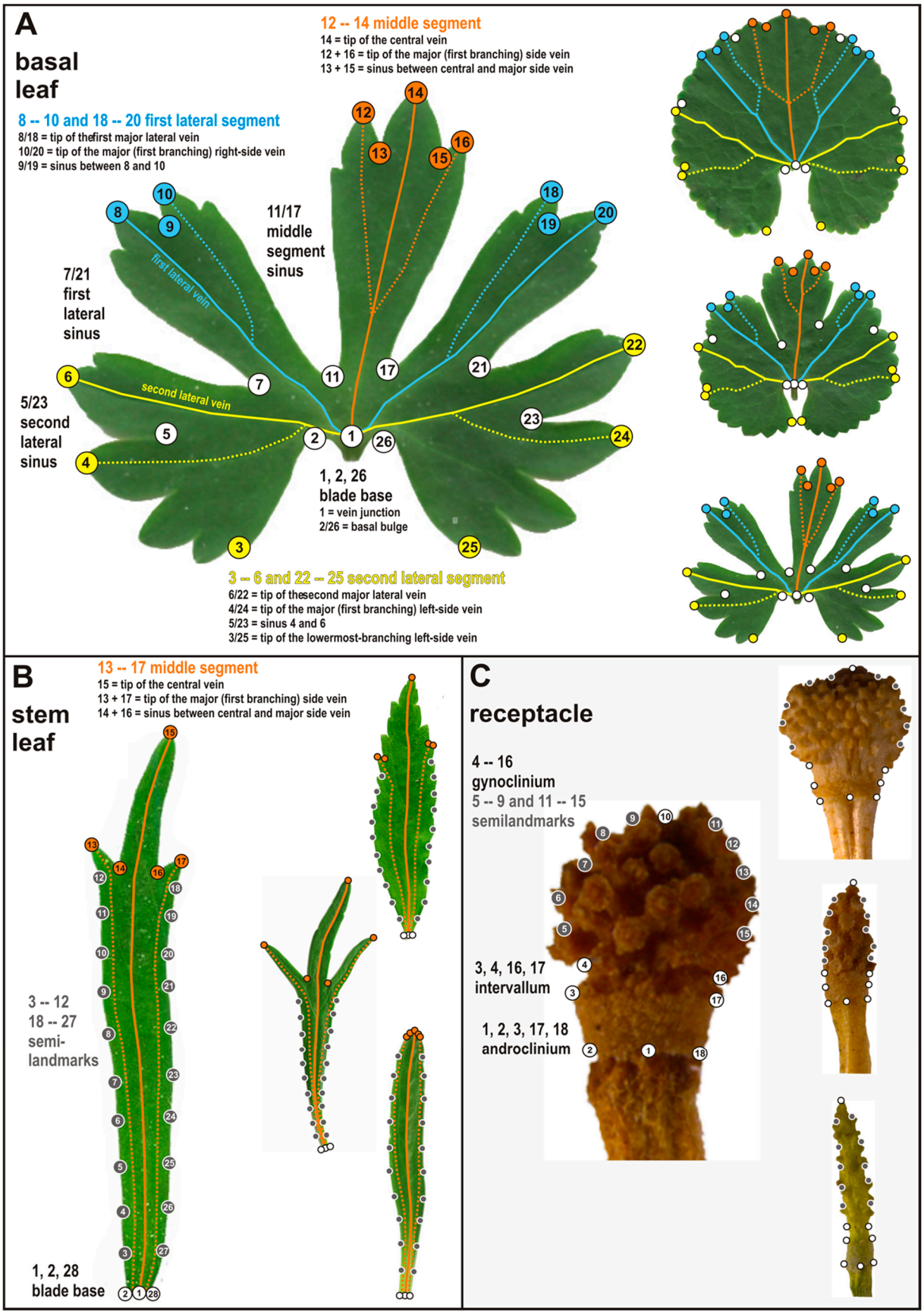

Figure S1. Landmark digitization of the taxonomically most informative *Ranunculus auricomus* traits. The original Figure was created by [1] (Figure S4 of [1]; published under Creative Commons Attribution License), and not modified herein. Original figure legend: '**(A)** Delimitation of 26 landmarks on basal leaf outline following homologous leaf venation pattern,

segments, and sinuses. **(B)** Delimitation of 8 landmarks (white and orange dots) and 20 semilandmarks (grey dots) on the stem leaf outline. **(C)** Delimitation of 8 landmarks (white dots) and 10 semilandmarks (grey dots) on the receptacle outline.'

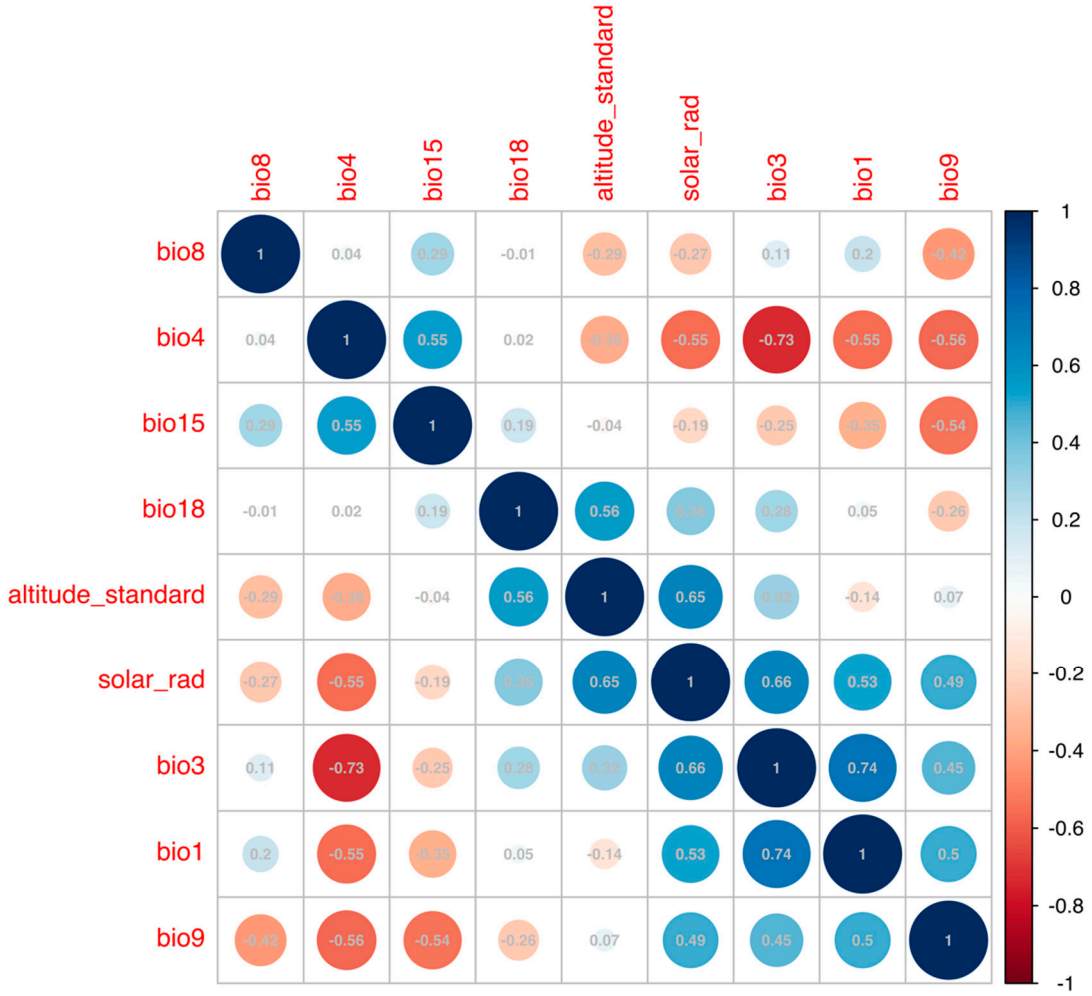

Figure S2. Correlation plot concerning non-autocorrelated (r<0.8), standardized (0 mean, unit variance) abiotic environmental factors. We used the package 'corrplot' vers. 0.92 [2] and the R version 4.2.0 [3] for calculating correlations. BIO1: annual mean temperature, BIO3: isothermality, BIO4: temperature seasonality, BIO8: mean temperature of wettest quarter, BIO9: mean temperature of driest quarter, BIO15: precipitation seasonality, BIO18: precipitation of warmest quarter, altitude_standard: altitude, and solar_rad: solar radiation. Concerning bioclimatic variables (and altitude and solar radiation), please see https://www.worldclim.org/data/bioclim.html for details.

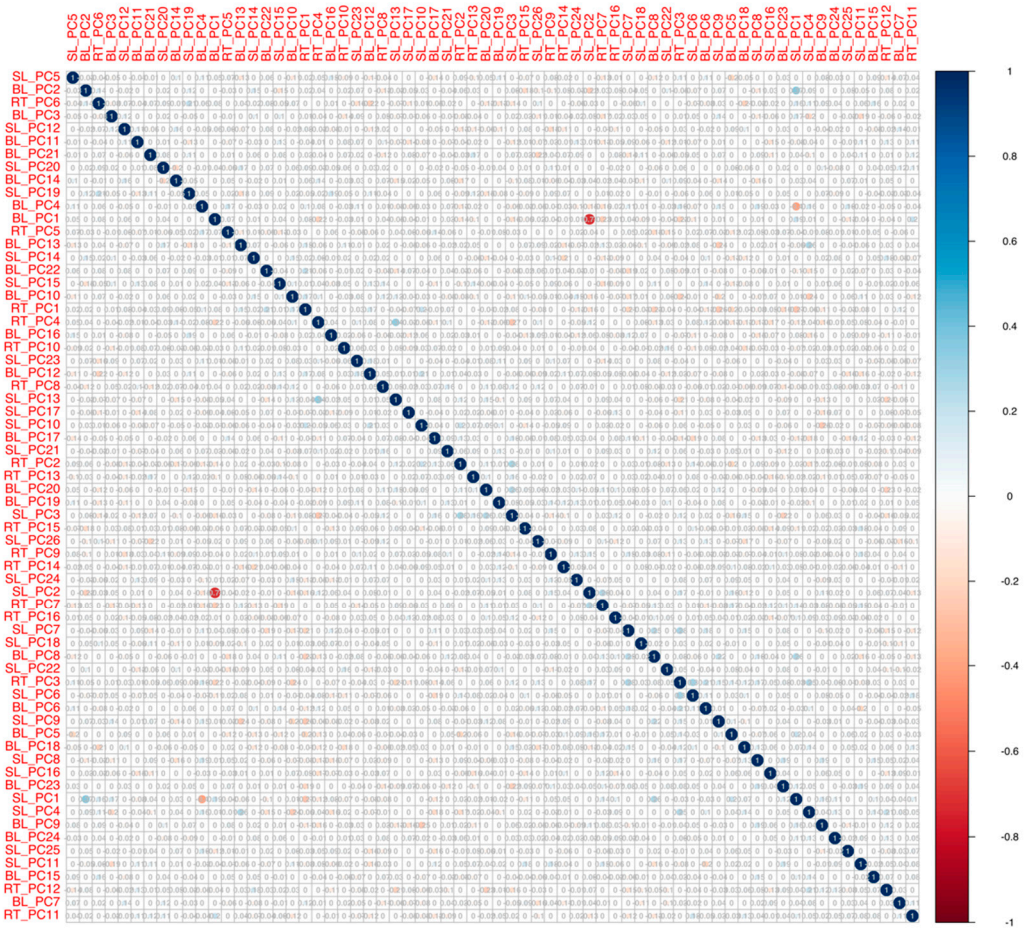

Figure S3. Correlation plot concerning standardized axis shape scores of all taxonomically informative traits. We used the package 'corrplot' vers. 0.92 [2] and the R version 4.2.0 [3] for calculating correlations. Some significant correlations were observed, but no autocorrelations ($r<0.8$). The only remarkable one is between BL PC1 (basal leaf ordination axis 1) and SL PC2 (stem leaf ordination axis 2).

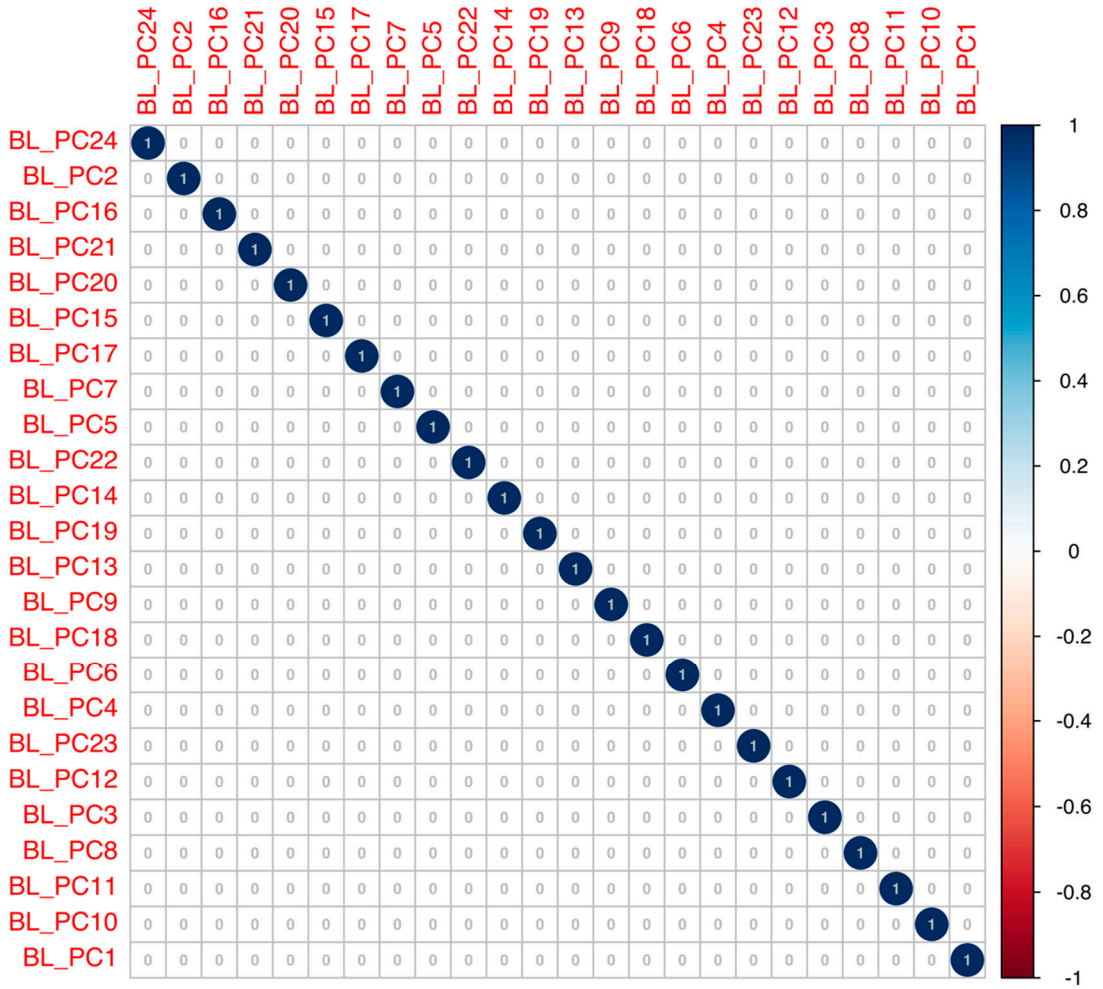

Figure S4. Correlation plot concerning standardized axis shape scores of basal leaves. We used the package 'corrplot' vers. 0.92 [2] and the R version 4.2.0 [3] for calculating correlations. No significant autocorrelations were observed.

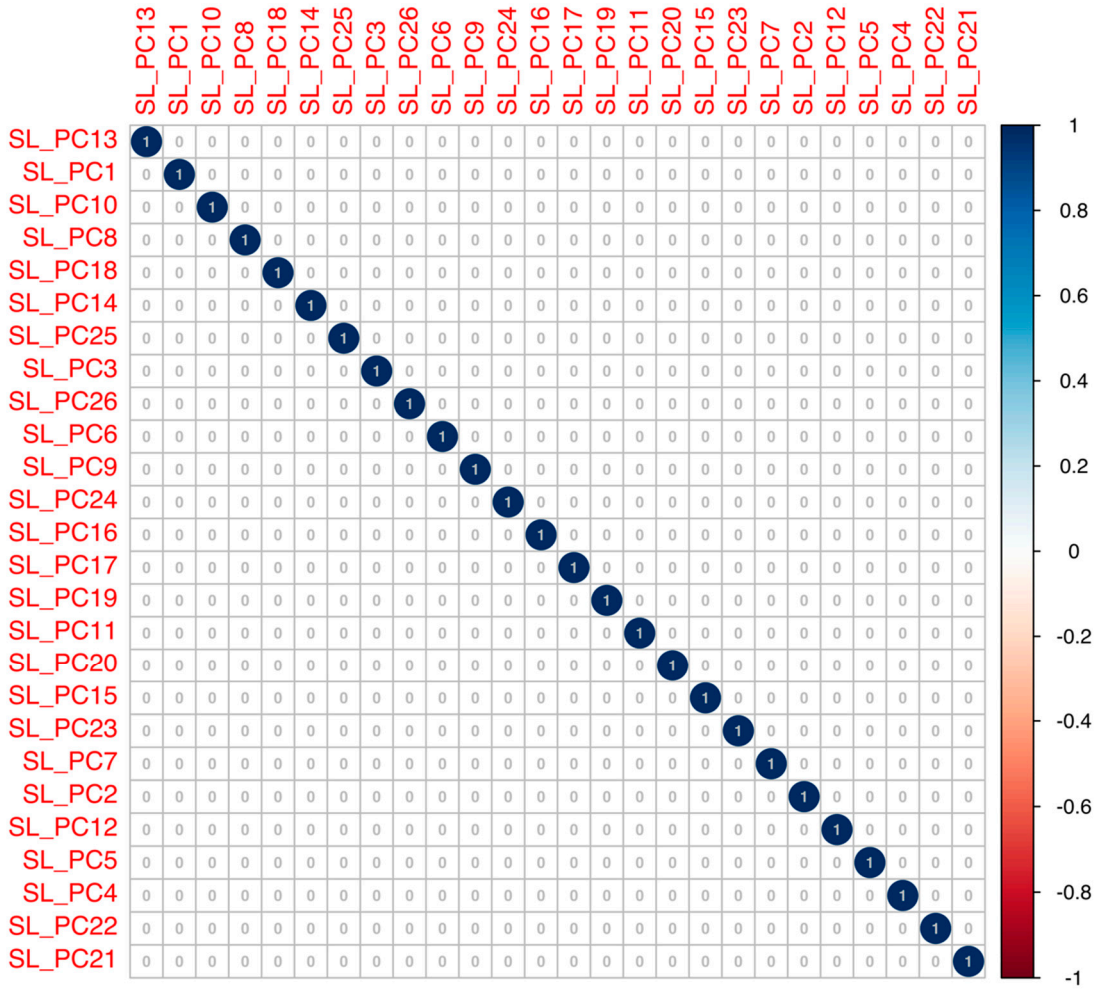

Figure S5. Correlation plot concerning standardized axis shape scores of stem leaves. We used the package 'corrplot' vers. 0.92 [2] and the R version 4.2.0 [3] for calculating correlations. No significant autocorrelations were observed.

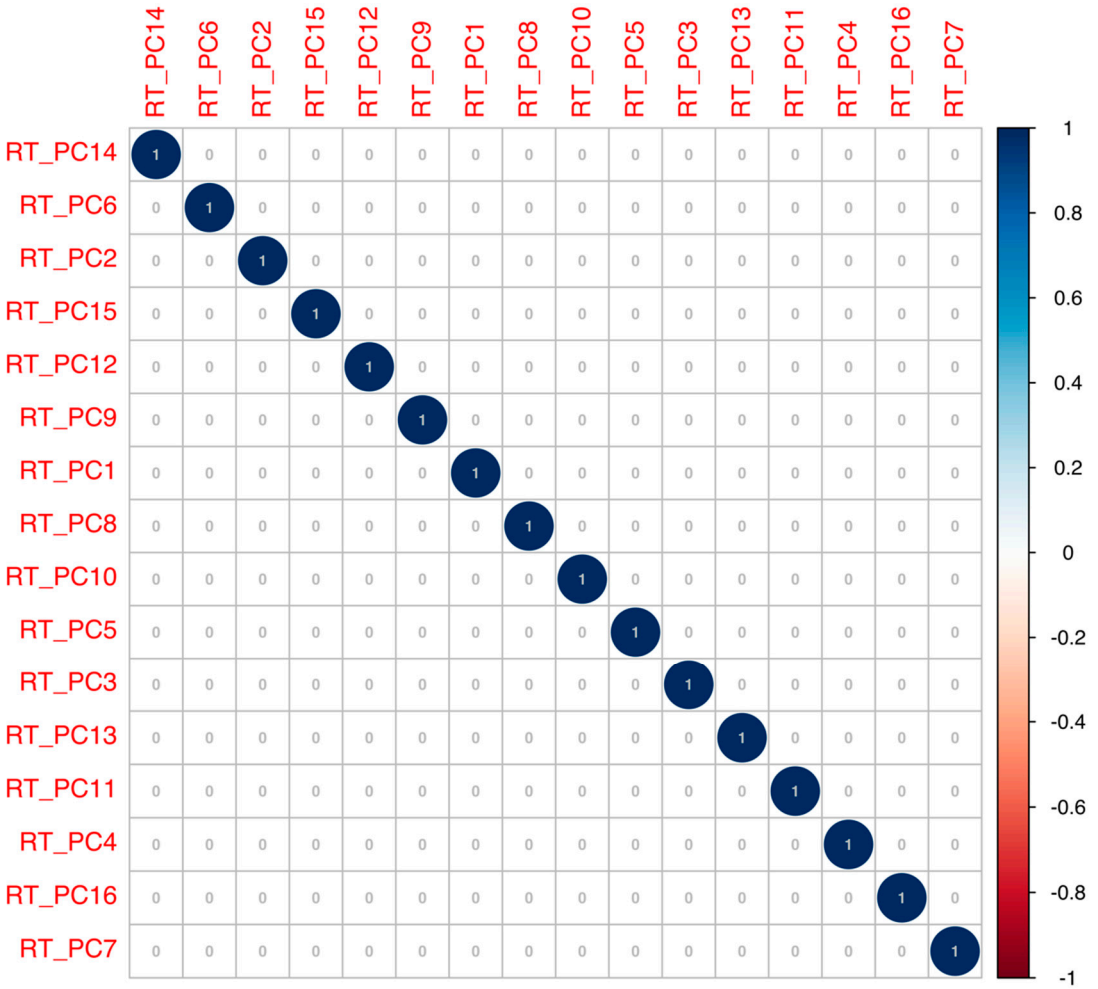

Figure S6. Correlation plot concerning standardized axis shape scores of receptacles. We used the package 'corrplot' vers. 0.92 [2] and the R version 4.2.0 [3] for calculating correlations. No significant autocorrelations were observed.

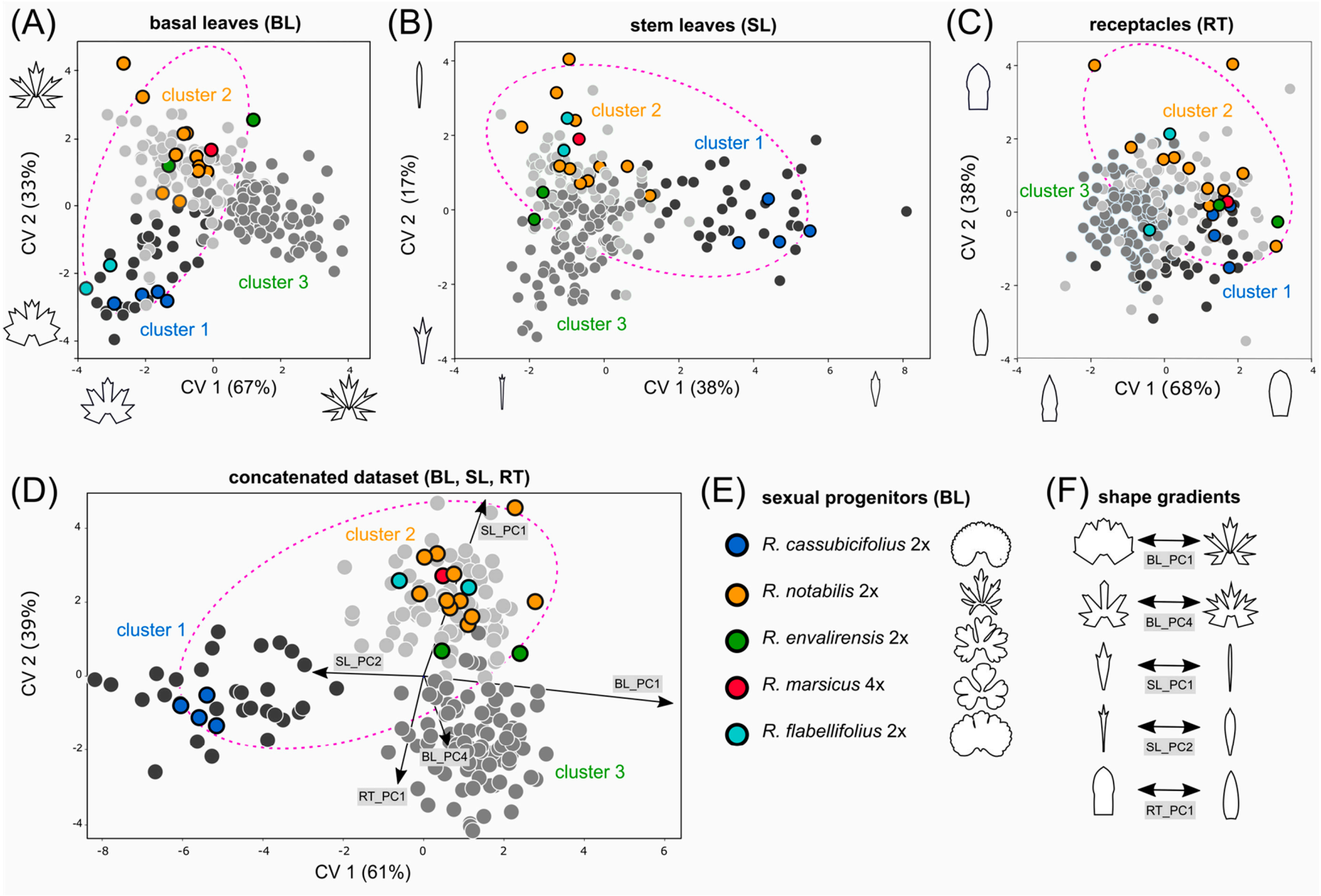
(A)
basal leaves (BL)
cluster 2
cluster 3
cluster 1
CV 2 (33%)
CV 1 (67%)
(B)
stem leaves (SL)
cluster 2
cluster 1
cluster 3
CV 2 (17%)
CV 1 (38%)
(C)
receptacles (RT)
cluster 2
cluster 3
cluster 1
CV 2 (38%)
CV 1 (68%)
(D)
concatenated dataset (BL, SL, RT)
cluster 2
SL_PC1
cluster 1
SL_PC2
BL_PC1
BL_PC4
cluster 3
RT_PC1
CV 2 (39%)
CV 1 (61%)
(E)
sexual progenitors (BL)
R. cassubicifolius 2x
R. notabilis 2x
R. envalirensis 2x
R. marsicus 4x
R. flabellifolius 2x
(F)
shape gradients
BL_PC1
BL_PC4
SL_PC1
SL_PC2
RT_PC1

Figure S7. Morphological variation among sexual progenitors and polyploid apomictic derivative taxa with respect to the genomic RAD-Seq (RADpainter) background. Canonical variates analyses (CVA) were applied for the clustering of 220 populations based on basal leaves **(A)**, stem leaves **(B)**, receptacles **(C)**, and the concatenation of all traits **(D)**. The concatenated analysis of all three traits (D) shows the five best separating morphometric trends illustrated in (F). Each dot in the CVA scatter plots (A-D) represents a single population, and the colors reflect assignments into the three RADpainter clusters (i.e., genomic clusters 1-3). An overview of the five sexual species in **(E)** shows their characteristic basal leaf morphotype, the most important taxonomic trait. The five best-separating shape trends (shape changes along the relative warps) are visualized in **(F)**. The coloring of sexual progenitors and clusters basically follows Fig. 2 and [4], but with different grey colors. Ellipses contain 95% of sexual progenitor populations. All polyploid apomictic populations outside these ellipses can be treated as 'transgressive morphotypes'. BL = basal leaves, Cluster 1 = RAD-Seq (RADpainter) cluster 1 containing *R. cassubicifolius* and polyploid apomictic relatives, Cluster 2 = RAD-Seq (RADpainter) cluster 2 containing *R. flabellifolius*, *R. marsicus*, and *R. notabilis* and polyploid apomictic relatives, Cluster 3 = RAD-Seq (RADpainter) cluster 3 containing *R. envalirensis* and polyploid apomictic relatives, CV = canonical variate (explained percentages of shape variation), SL = stem leaves, RT = receptacles.

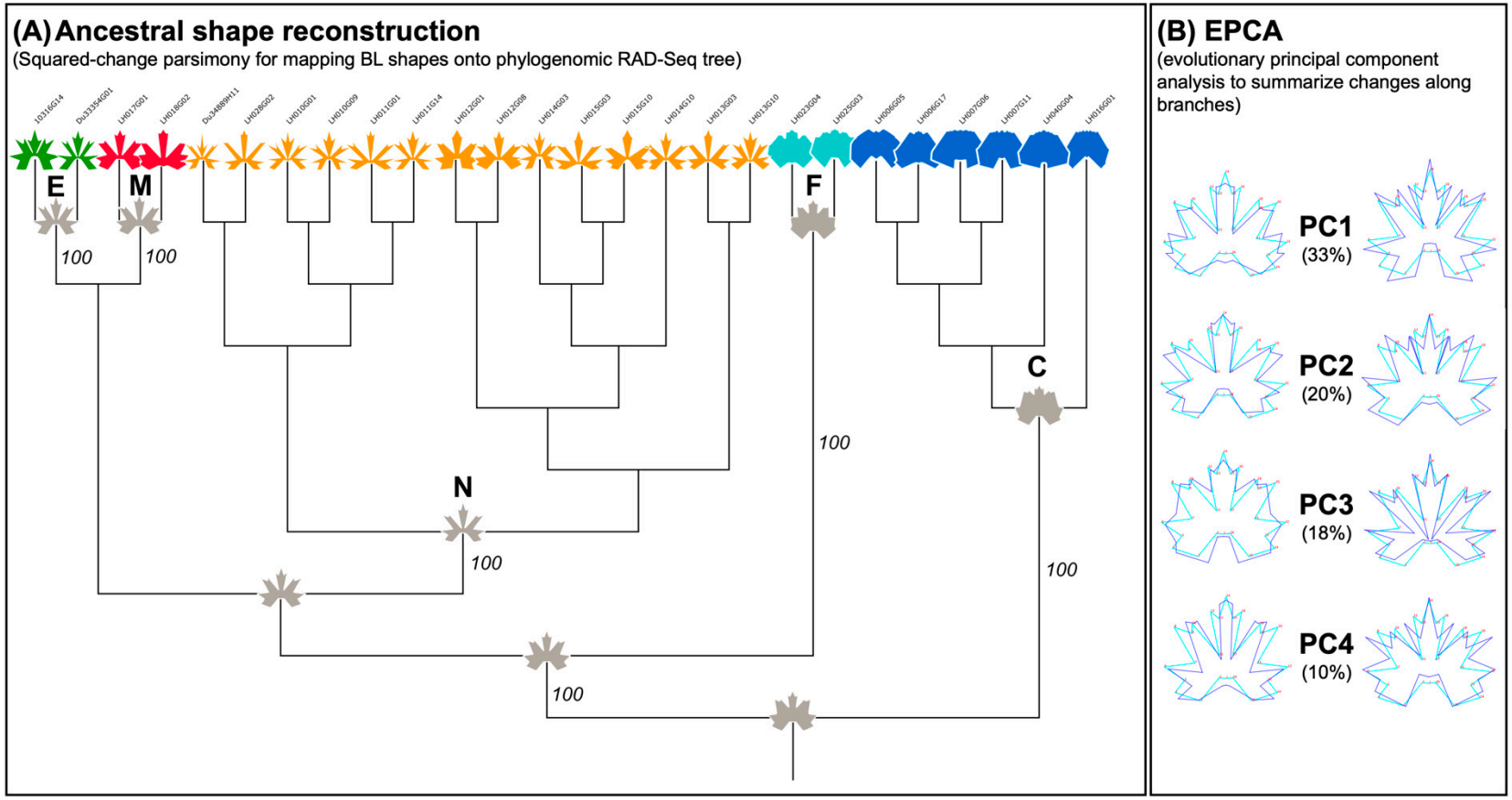

Figure S8. Ancestral BL shape reconstruction using the sexual progenitors. **(A)** Squared-change parsimony reconstruction for mapping BL shapes onto a phylogenomic ML tree (RAD-Seq; 93,924 loci, 85,849 SNPs, 67% missing data; IPYRAD and RAxML_NG analysis followed [1,4]) to reconstruct the main morphological shifts of basal leaves. Colorized basal leaf silhouettes on branch tips represent mean BL shapes (averaged across plant individuals). The grey basal leaf silhouettes represent the reconstructed BL shapes at selected nodes. E=*R. envalirensis* (green), M=*R. marsicus* (red), N=*R. notabilis* (orange), F=*R. flabellifolius* (turquoise), C=*R. cassubicifolius* (blue). **(B)** Evolutionary principal components analysis (EPCA) to summarize and visualize the main changes along all the branches in the phylogeny **(A)**.

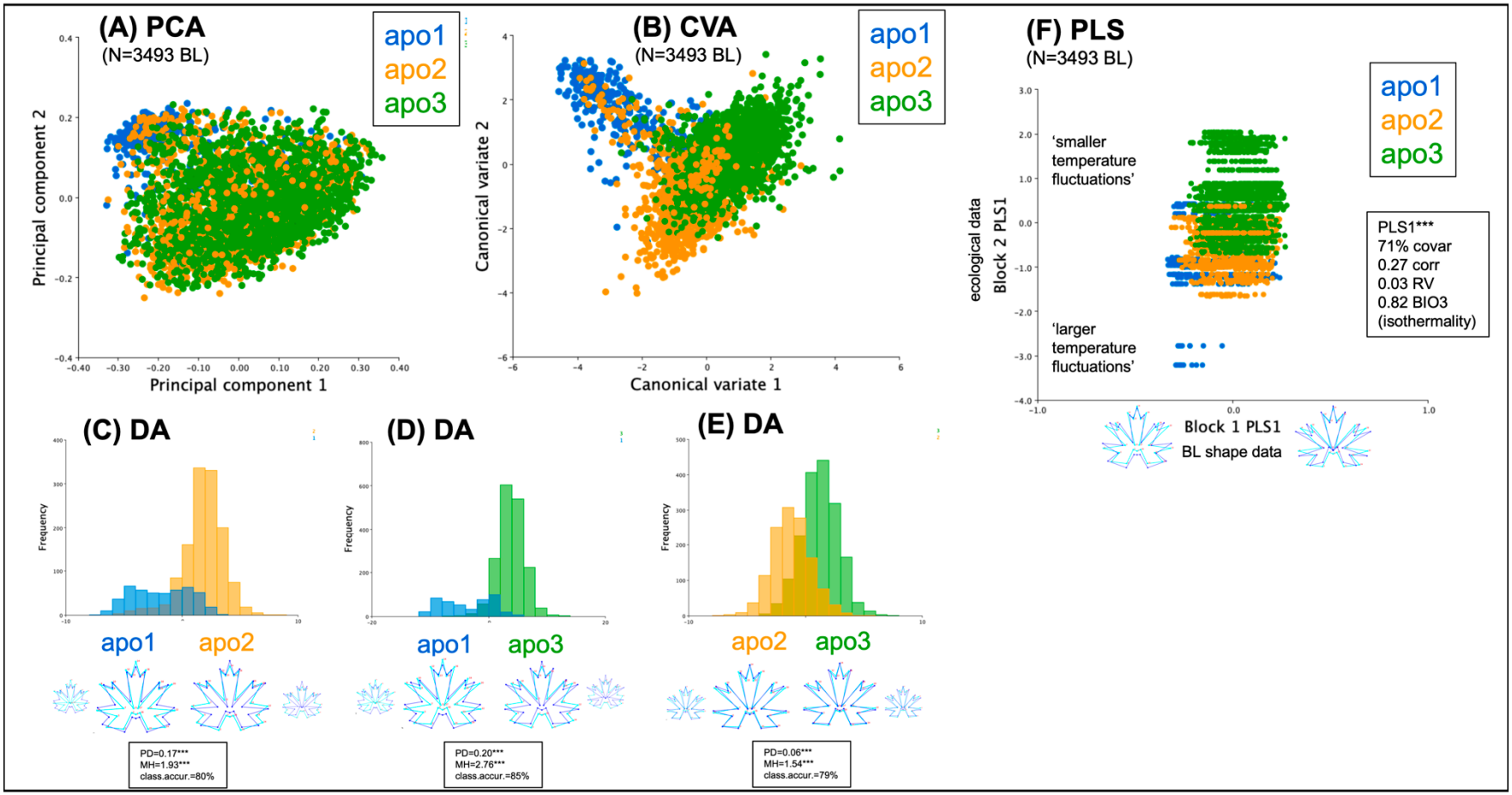

Figure S9. Basal leaf (BL) differentiation among clusters: apomictic polyploids. Morphological variation of basal leaf shapes in polyploid apomicts. **(A)** Principal component analysis (PCA) of 3493 basal leaf landmark configurations colorized according to the three RAD-Seq clusters 1-3. **(B)** Canonical variates analysis (CVA) of the same data as in **(A)** with predefined groups (clusters 1-3). **(C)** Discriminant analysis (DA) of basal leaves from clusters 1 and 2 (only apomictic polyploids). **(D)** Discriminant analysis (DA) of basal leaves from clusters 1 and 3 (only apomictic polyploids). **(E)** Discriminant analysis (DA) of basal leaves from clusters 2 and 3 (only apomictic polyploids). **(F)** Partial least squares analysis (PLS) of covariance between the basal leaf shapes (across the three clusters) and four ecological variables significantly associated with phenotypic variation of BL.

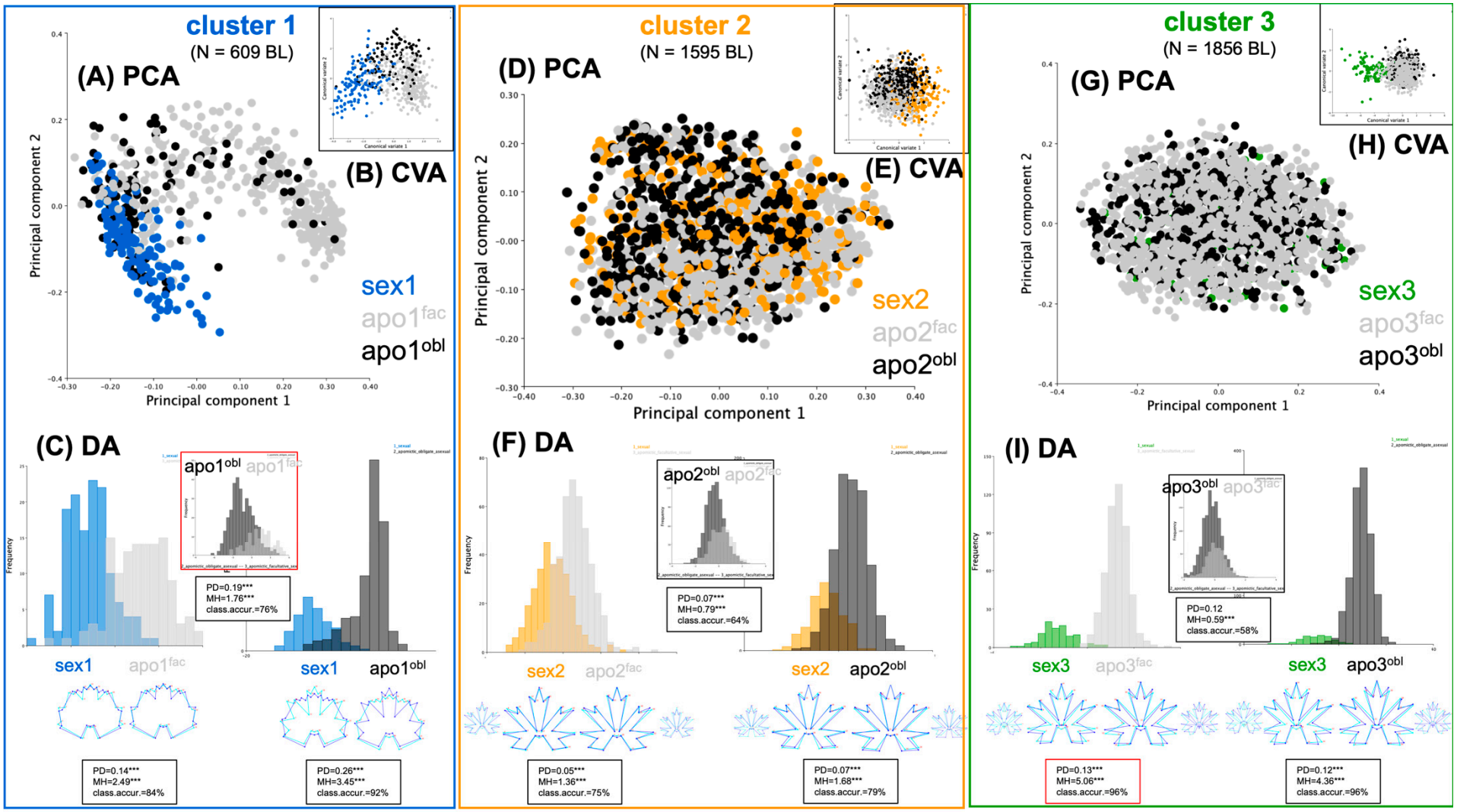

Figure S10. Basal leaf (BL) differentiation within clusters: sexuals vs. apomicts. Comparison of morphological variation among the apomictic polyploids and sexual species. **(A)-(C)** cluster 1, **(D)-(F)** cluster 2, **(G)-(I)** cluster 3. **(A)** Principal component analysis (PCA) of 609 basal leaves from the cluster 1; blue=sexual *R. cassubicifolius* (sex), grey=facultative apomicts (apo^{fac}), black=obligate apomicts (apo^{obl}). **(B)** Canonical variate analysis

(CVA) of the BL shapes from the three predefined groups. **(C)** Discriminant analysis (DA) of the BL shapes from pairs of predefined groups (sexual *R. cassubicifolius* vs. facultative apomicts, sexual *R. cassubicifolius* vs. obligate apomicts, facultative apomicts vs. obligate apomicts. **(D)** Principal component analysis (PCA) of 1595 basal leaves from cluster 2; orange=sexual *R. notabilis/R. flabellifolius/R. marsicus* (sex), grey=facultative apomicts (apo^{fac}), black=obligate apomicts (apo^{obl}). **(E)** Canonical variate analysis (CVA) of the BL shapes from the three predefined groups. **(F)** Discriminant analysis (DA) of the BL shapes from pairs of predefined groups as described in **(D)**. **(G)** Principal component analysis (PCA) of 1856 basal leaves from the cluster 3; green=sexual *R. envalirensis* (sex), grey=facultative apomicts (apo^{fac}), black=obligate apomicts (apo^{obl}). **(H)** Canonical variate analysis (CVA) of the BL shapes from the three predefined groups. **(I)** Discriminant analysis (DA) of the BL shapes from pairs of predefined groups as described in **(G)**.

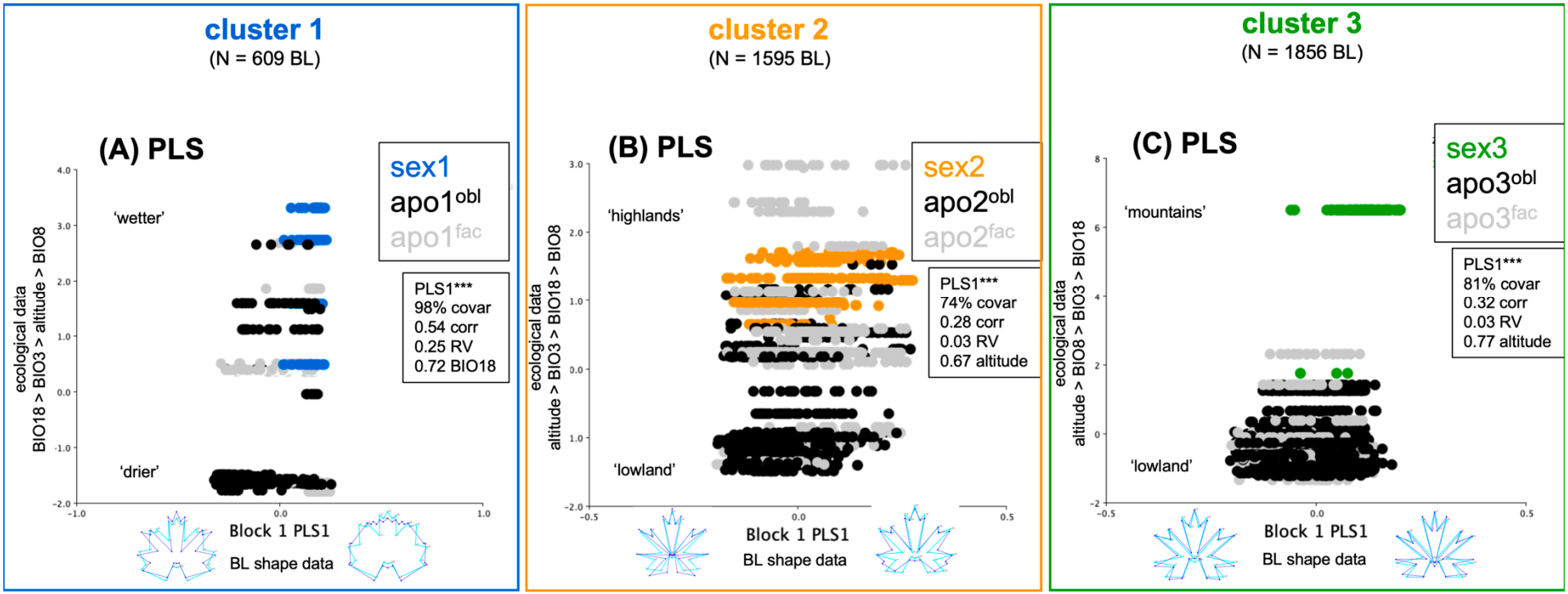

Figure S11. Basal leaf (BL) differentiation within clusters: ecological covariance. Partial least squares analysis (PLS) of covariance between BL shape variation and ecological variables. **(A)** PLS analysis of the sexual *R. cassubicifolius* (blue dots) and apomicts (grey and black dots) from cluster 1 - evaluation of the relative importance of the four ecological variables (altitude, BIO3, BIO8, BIO18), which significantly covary with BL shape variation (Block 1 PLS1). The ecological variable with the highest PLS coefficient (0.72) for the first PLS axis represents BIO18 (precipitation of the warmest quarter). The graph shows that within cluster 1, the sexuals (blue) tend to have less dissected leaf phenotypes (Block 1 PLS1) and prefer a wetter climate, whereas the apomicts are shifted towards a drier climate and tend to have less dissected leaves (especially the obligate apomicts; black dots). **(B)** PLS analysis of the sexual *R. notabilis*/*R. flabellifolius*/*R. marsicus* (orange dots) and apomicts (grey and black dots) from cluster 2 - evaluation of the relative importance of the four ecological variables (altitude, BIO3, BIO8, BIO18), which significantly covary with BL shape variation. The ecological variable with the highest PLS coefficient (0.67) for the first PLS axis was found to be altitude. The graph shows that within cluster 2 the sexuals (orange dots) and apomicts have a similar range of BL shape variation (Block 1 PLS1), whereas the sexuals rather prefer a

'highland' climate (mountainous regions around 500 m. a. s. l.), the obligate apomicts (black dots) tend to prefer lowland climate. A couple of facultative apomicts (grey dots) also exploit higher altitudes compared to sexuals. **(C)** PLS analysis of the sexual *R. envalirensis* (green dots) and apomicts (grey and black dots) from cluster 3 - evaluation of the relative importance of the four ecological variables (altitude, BIO3, BIO8, BIO18), which significantly covary with BL shape variation (Block 1 PLS1). The ecological variable with the highest PLS coefficient (0.77) for the first PLS axis was found to be altitude. The graph shows that within cluster 3 the sexuals and apomicts differ in their BL shape variation (Block 1 PLS1), whereas the sexuals (green dots) prefer rather highland/alpine (> 1000 m a. s. l.) climate, and the apomicts (grey and black dots) tend to prefer lowland climate.

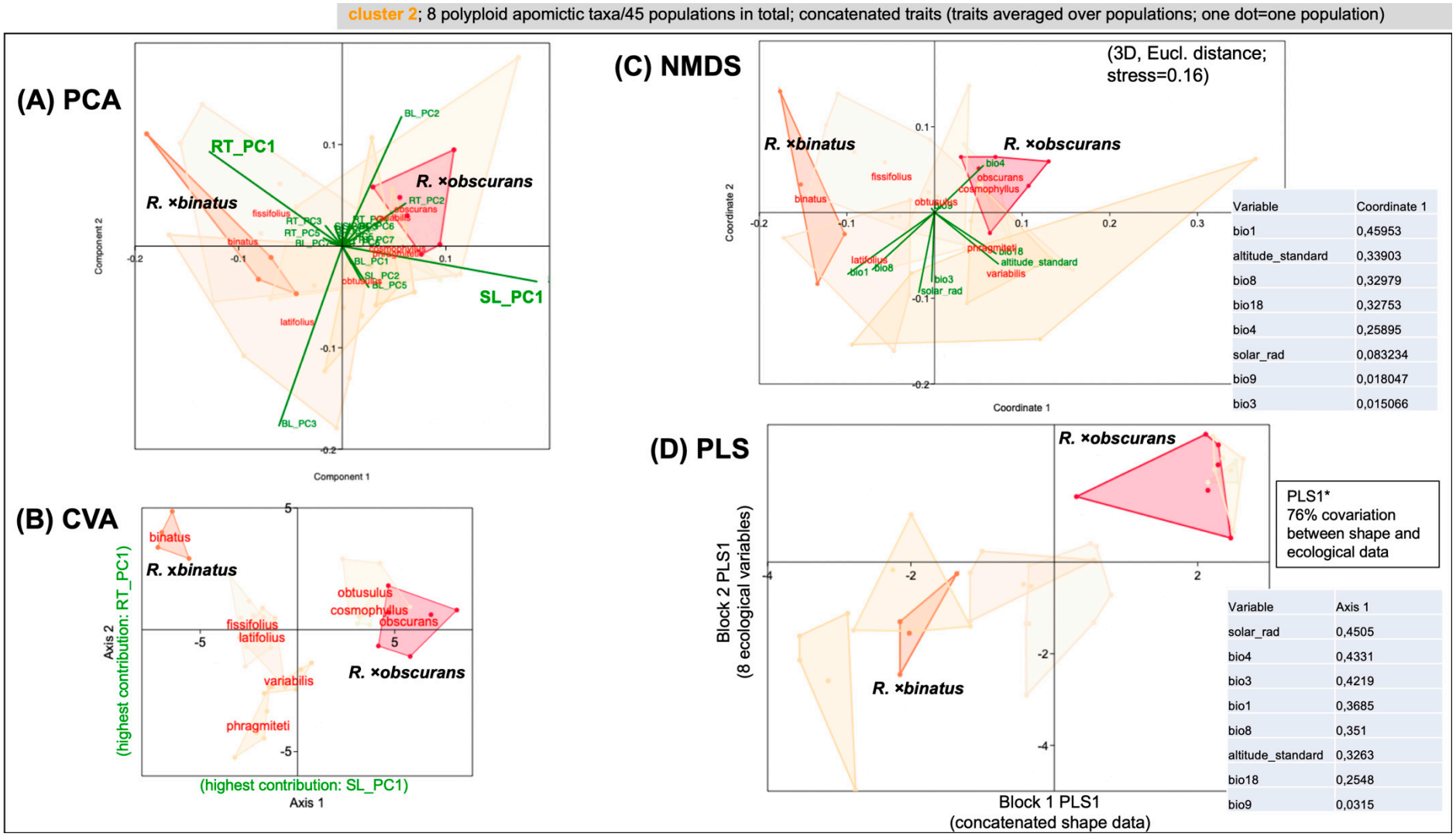

Figure S12. Morphological differentiation among apomictic polyploids. Multivariate analyses of the concatenated traits from eight apomictic polyploid taxa within cluster 2 (eight polyploid apomictic taxa/45 populations in total; concatenated traits - traits averaged over populations; one

dot=one population). Highlighted are two taxa that consistently show morphological separation from each other: *R.* ×*binatus* (four populations, obligate and facultative apomicts) and *R.* ×*obscurans* (eight populations, obligate and facultative apomicts). **(A)** Principal components analysis (PCA) of the concatenated traits from the eight apomictic polyploids from cluster 2. Stem leaf principal component 1 (SL_PC1) and receptacle principal component 1 (RT_PC1) are the two shape variables with the highest contribution to the component 1. **(B)** Canonical variates analysis (CVA) revealed that the shape variable best separating between *R.* ×*binatus* and *R.* ×*obscurans* was the stem leaf principal component 1 (SL_PC1; highest contribution to Axis 1, shape variable vector not shown). **(C)** Non-metric multidimensional scaling (3D) of the concatenated traits using Euclidean distance and fitted environmental variables. Mean annual temperature (BIO1) and altitude contribute the most to Coordinate 1. The Shepard stress for the given ordination was 0.1604. **(D)** Partial least squares analysis (PLS) depicted solar radiation, temperature seasonality (BIO4) and isothermally (BIO3) as the environmental variables with highest contributions to the first ordination axis (PLS 1) of the covariation between shape variables and environmental variables.

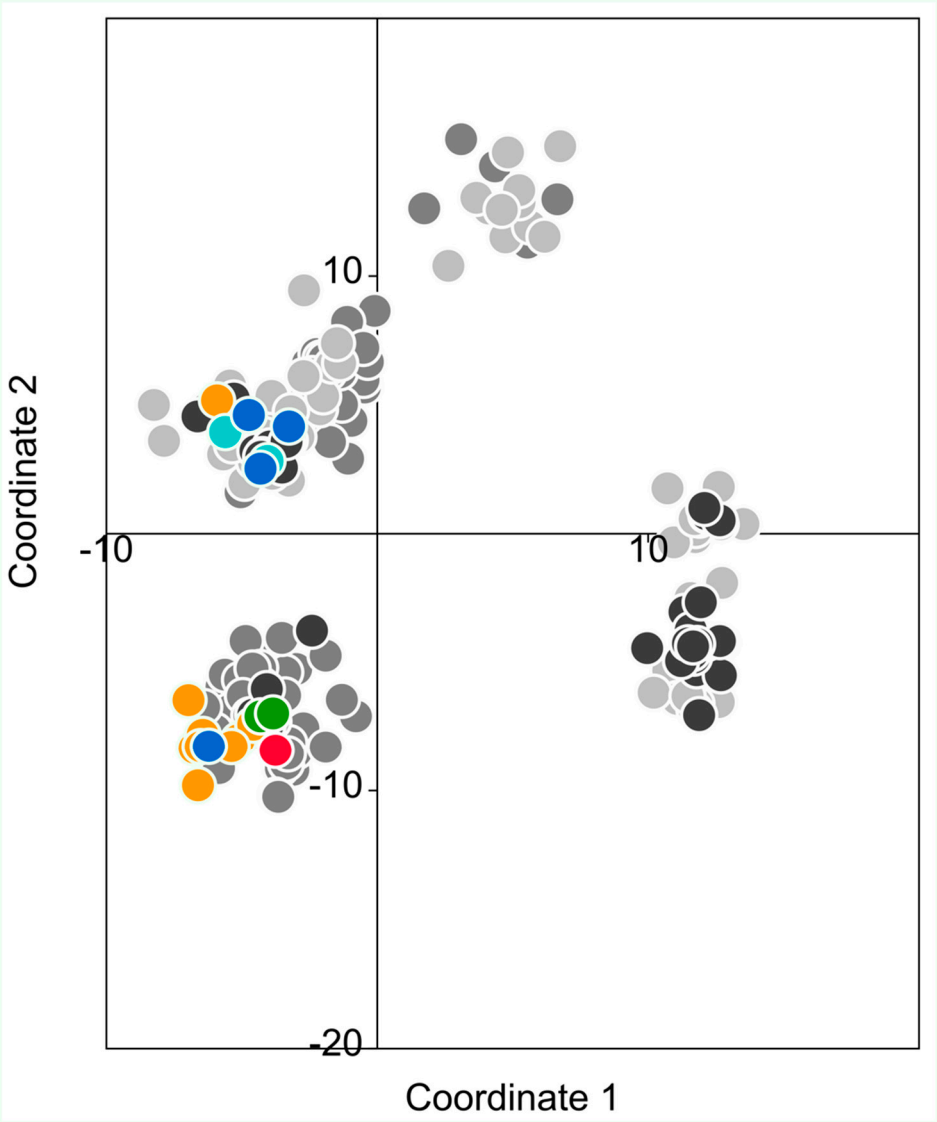

Figure S13. Ecological clustering of sexual and apomictic populations. Uniform manifold approximation (UMAP) ordination plot based on eight environmental variables. Each dot represents one population; cluster 1 apomicts: dark grey, cluster 2 apomicts: light grey, cluster 3 apomicts: grey, *R. cassubicifolius*: blue, *R. notabilis*: orange, *R. envalirensis*: green, *R. marsicus*: red, *R. flabellifolius*: turquoise.

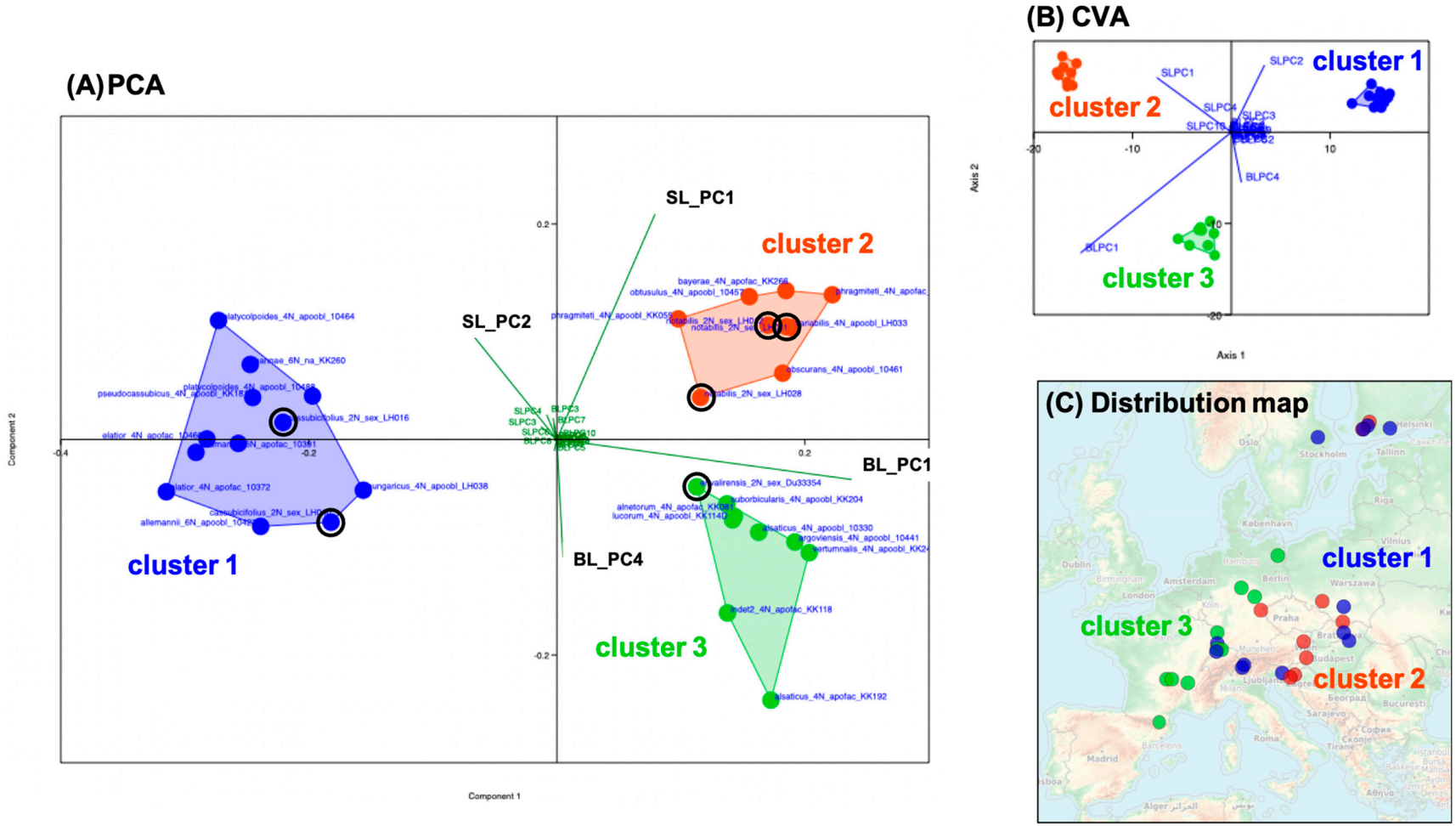

Figure S14. Selected sexuals and apomicts showing consistent genetic+morphological clusterings. **(A)** Principal components analysis (PCA) of 30 averaged population shape data (BL/10 shape variables, SL/10 shape variables) belonging to clusters 1-3 (in all RAD-Seq+TEG+CP analyses). **(B)** Canonical variate analysis (CVA) of the same data as in (A); the mean jackknifed classification accuracy =100%. **(C)** Distribution map of the populations analyzed in (A) and (B). See section 2.2.7 for more details. Blue dots: sexuals and apomicts of cluster 1, red dots: sexuals and apomicts of cluster 2, green dots: sexuals and apomicts of cluster 3; black circles in (A) highlight the sexuals.

Supplementary Materials

Tables S1-S7

Table S1. Information on 220 populations with complete evidence of collection (GPS), morphometric (BL+SL+RT), and genomic/RAD-Seq clustering data. The metadata is structured into six different sections as follows: MAJOR_GROUPS (=RAD-Seq/RADpainter clusters), IDENTIFIERS (population, individual plant, etc.), BIOLOGY (ploidy, reproduction mode, etc.), GENOMICS (RAD-Seq/TEG/CP clusterings), ECOLOGY (GPS, bioclimatic variables, etc.), and MORPHOMETRICS (original 2D landmark x,y-coordinates). Each row of the table corresponds to one measurement (=one morphometric object, i.e., the configuration of landmarks; please note that the number of landmarks differs among the three traits). Voucher specimens have been deposited in the herbarium of the University of Göttingen (GOET).

Table S2. Discriminant analysis of the differentiation among genomic (RAD-Seq), nuclear (TEG), and plastid (CP) clusters based on pairwise comparisons of single morphological traits and concatenated data. P-values below 0.05 are highlighted in green.

Table S3. Discriminant analysis of the differentiation among the three genomic (RAD-Seq) clusters based on pairwise comparisons of single morphological traits and concatenated data. BL = basal leaf, SL = stem leaf, RT = receptacle, CC = concatenated dataset, F = F-value (NPMANOVA). *** = Bonferroni corrected p-value < 0.001.

Table S4. Discriminant analysis of the differentiation among selected nothotaxa within each of the three genomic (RAD-Seq) clusters based on pairwise comparisons of the three morphological traits. P-values below 0.05 are highlighted in green.

Table S5. Regression models of the association between genomic contributions of the sexual species and shape variation in apomictic polyploids (mostly allopolyploids). C=*R. cassubicifolius*, E=*R. envalirensis*, N=*R. notabilis*.

Table S6. Distance matrix-based multiple regression models (MRM) to explain the source of shape variation. We used 211 populations characterized by shape, abiotic environmental, and genomic RAD-Seq (RADpainter) information. MRMs are based on scaled (unit variance) variables, and we specified 1000 permutations and Spearman rank correlations due to non-normally distributed data. The following MRMs were calculated: (i) A general model using shape distances as response and environmental and genomic distances (and their interaction) as explanatory variables, and (ii-iv) three detailed models using shape distances of basal leaves (BL), stem leaves (SL), and receptacles (RT) as the response variable and all single environmental factor (BIO3-18, solar radiation, and altitude) and genomic distances. The regression estimates specify the slope and direction of the regression (significant ones, $p<0.05$, highlighted in bold). BL = basal leaf, D = distance, morph. = morphological (shape), SL = stem leaf, RT = receptaculum, R^2 = Coefficient of determination (% of explained variance).

Table S7. Regression models of the association between eight non-correlated ecological predictors and variation of all three morphological traits. The eight ecological predictors were selected in previous analyses and are significantly associated with shape variation.

References

1. Karbstein, K.; Tomasello, S.; Hodač, L.; Dunkel, F.G.; Daubert, M.; Hörandl, E. Phylogenomics Supported by Geometric Morphometrics Reveals Delimitation of Sexual Species within the Polyploid Apomictic *Ranunculus auricomus* Complex (Ranunculaceae). *Taxon* **2020**, *69*, 1191–1220, doi:10.1002/tax.12365.
2. Taiyun, W.; Simko, V. Corrplot - Visualization of a Correlation Matrix 2022.
3. R Core Team R: A Language and Environment for Statistical Computing 2022.
4. Karbstein, K.; Tomasello, S.; Hodač, L.; Wagner, N.; Marinček, P.; Barke, B.H.; Paetzold, C.; Hörandl, E. Untying Gordian Knots: Unraveling Reticulate Polyploid Plant Evolution by Genomic Data Using the Large *Ranunculus auricomus* Species Complex. *New Phytol.* **2022**, *235*, 2081–2098, doi:10.1111/nph.18284.